Medicinal Chemistry Research (2018) 27:2016–2026
https://doi.org/10.1007/s00044-018-2210-0

MEDICINAL CHEMISTRY RESEARCH

ORIGINAL RESEARCH

Antioxidant and anti-inflammatory oxygenated meroterpenoids from the thalli of red seaweed *Kappaphycus alvarezii*

Fasina Makkar[1,2] · Kajal Chakraborty[1]

Received: 25 February 2018 / Accepted: 22 June 2018 / Published online: 2 July 2018

Abstract

Three antioxidant and anti-inflammatory oxygenated meroterpenoids, 1-(3-methoxypropyl)-2-propylcyclohexane (C_{13}) (**1**), 3-(methoxymethyl)heptyl 3-(cyclohex-3-enyl) propanoate (C_{18}) (**2**), and 2-ethyl-6-(4-methoxy-2-((2-oxotetrahydro-2*H*-pyran-4-yl)methyl)butoxy)-6-oxohexyl 5-ethyloct-4-enoate (C_{29}) (**3**) were purified from the methanol:ethyl acetate fraction of red seaweed *Kappaphycus alvarezii* (family Solieriaceae) collected from the Gulf-of-Mannar on the southeast coast of peninsular India. The highly oxygenated C_{29} meroterpenoid **3** displayed potential antioxidative activities ($IC_{50} < 0.35$ mg/mL) as evaluated by 2, 2'-azino-bis (3-ethylbenzothiazoline)-6-sulphonic acid and 1, 1-diphenyl-2-picryl-hydrazil free radical scavenging assays. The compound **3** displayed potential *in vitro* inh*i*bitory activities towards pro-inflammatory 5-lipoxidase (IC_{50} 1.04 mg/mL), which indicated its potential anti-inflammatory properties against inducible inflammatory mediators causing an inflammatory response. Structure-activity relationship analyses displayed the functional roles of lipophilic-hydrophobic characteristics and electronic parameter to determine its potential anti-inflammatory activity in terms of inhibiting inducible inflammatory cyclooxygenase and lipoxidase.

Keywords *Kappaphycus alvarezii* · Solieriaceae · Oxygenated C_{29} meroterpenoid · Antioxidant · Anti-inflammatory activity · Inducible inflammatory mediators

Introduction

Terpenoids are structurally diverse secondary metabolites with more than 40,000 reported structural diversity possessing valuable bioactive properties (Gershenzon and Dudareva 2007). Terpenoids were recognized to possess potential pharmacological properties against deadly diseases, such as malaria (Parshikov et al. 2012), cardiovascular ailments (Liebgott et al. 2000) and cancer (Ebada et al. 2010). Seaweeds or marine macroalgae were found to be the potential reservoir of bioactive secondary metabolites including terpenes, sterols, polyphenols, acetogenins, etc. (Reis et al. 2013), and the most prominent among these are meroterpenoid group of compounds (Chakraborty et al. 2016). A rare meroterpenoid (secotaondiol) with potential gastroprotective activity was described in a previous report of literature (Areche et al. 2015). The meroditerpene, 11-hydroxy-11-*O*-methylamentadione, isolated from the seaweed *Cystoseira usneoides* showed anti-inflammatory effects in dextran sodium sulphate-persuade colitis in a murine model. The terpenoid compound was found to significantly inhibit the generation of the cytokine (a type of inflammatory signaling molecule) and tumour necrosis factor in lipopolysaccharide-induced human monocytic leukaemia cell line (Zbakh et al. 2016). Three antioxidative aryl meroterpenoids were previously isolated from the red seaweed *Hypnea musciformis* (Chakraborty et al. 2016).

Among different red seaweeds, *Kappaphycus alvarezii* (Doty) (family Solieriaceae) is a commercially important and cultivable species that is predominantly abundant in

These authors contributed equally: Fasina Makkar and Kajal Chakraborty

Electronic supplementary material The online version of this article (https://doi.org/10.1007/s00044-018-2210-0) contains supplementary material, which is available to authorized users.

✉ Kajal Chakraborty
kajal_cmfri@yahoo.com
kajal.chakraborty@icar.gov.in

[1] Marine Bioprospecting Section of Marine Biotechnology Division, Central Marine Fisheries Research Institute, Ernakulam North, P. B. No. 1603, Cochin, India

[2] Department of Chemistry, Mangalore University, Mangalagangothri, Mangalore, Karnataka State 574199, India

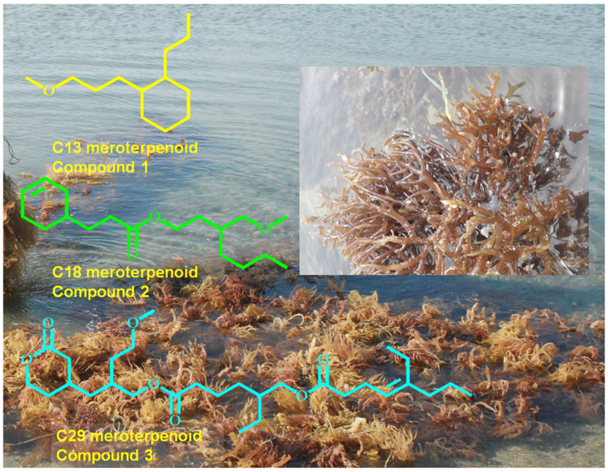

Fig. 1 Oxygenated meroterpenoids, 1-(3-methoxypropyl)-2-propylcyclohexane (**1**), 3-(methoxymethyl)heptyl 3-(cyclohex-3-enyl)propanoate (**2**) and 2-ethyl-6-(4-methoxy-2-((2-oxotetrahydro-2*H*-pyran-4-yl)methyl)butoxy)-6-oxohexyl 5-ethyloct-4-enoate (**3**) isolated from red seaweed *K. alvarezii*. The thalli of the studied seaweed were displayed as inset

tropical coastal and marine habitats in the southeast Asian countries, especially Malaysia, India, Indonesia, Philippines, China and Taiwan (Chandrasekaran et al. 2008; Ask and Azanza 2002). We have previously described the anti-inflammatory and antioxidant potentials of unprecedented cyclic ether along with pharmacologically active polygalactan from this seaweed species (Makkar and Chakraborty 2017a; Makkar and Chakraborty 2017b, c). The present study aimed to isolate three specialized oxygenated meroterpenoids, 1-(3-methoxypropyl)-2-propylcyclohexane (C_{13}) (**1**), 3-(methoxymethyl)heptyl 3-(cyclohex-3-enyl)propanoate (C_{18}) (**2**) and 2-ethyl-6-(4-methoxy-2-((2-oxotetrahydro-2*H*-pyran-4-yl)methyl)butoxy)-6-oxohexyl 5-ethyloct-4-enoate (C_{29}) (**3**) of *K. alvarezii* collected from the shallow marine habitats of the Gulf-of-Mannar on the south-east coast of Peninsular India (Fig. 1). The anti-inflammatory and antioxidative activities of these compounds were evaluated by different *in vitro* models and their structures were proposed on the basis of 2D-NMR experiments. The physicochemical characteristics of meroterpenoids contributing towards the antioxidant and anti-inflammatory activities were ascertained by structure-activity relationship analyses.

Materials and methods

Chemicals and instrumentation

FTIR spectral data were recorded in Perkin–Elmer Series 2000 (scan range of 400 and 4000 cm^{-1}). A Varian Cary 50 Uv–vis spectrometer (Varian Cary, USA) was utilized to acquire the UV spectral data. Two-dimensional NMR spectral experiments were performed on a Bruker Avance DPX 500 (500 MHz) spectrometer ($CDCl_3$ as aprotic solvent). Standard pulse sequences were used for HMBC, HSQC, ^{1}H–^{1}H COSY, NOESY, and DEPT experiments. GC-MS analyses were carried out with an EI mode {Varian GC (CP-3800) housed in a mass spectrometer (Varian 1200 L)}. ESI-MS data were obtained by using a liquid chromatography-mass spectrometry system (Applied Biosystems QTrap 2000, Germany). The solvents used for analyzing samples were of analytical grade (E-Merck, Germany).

Collection of seaweed samples of *K. alvarezii* and extraction

The red seaweed *K. alvarezii* were freshly collected from the Gulf of Mannar in Mandapam region located between 8° 48′ N, 78°9′ E and 9°14′ N, 79°14′E on the southeast coast of India. The seaweed thalli were washed in running water for 15 min and shade dried (~36 °C, 36 h). The shade dried seaweed thalli were ground before being extracted (1 kg) with solvent methanol: ethyl acetate (3 h, 1:1, v/v, 60–70 ° C) before being dried through anhydrous Na_2SO_4. The pooled filtrate was concentrated below 50 °C by using a rotary vacuum evaporator (Heidolph, Germany) to dryness to yield a dark brown residue of crude ethyl acetate-methanol (EtOAc: MeOH) fraction of *K. alvarezii* (45 g, yield on dry basis 4.5%).

Purification of meroterpenoids from the red seaweed *K. alvarezii*

The crude EtOAc: MeOH fraction of *K. alvarezii* (20 g) was loaded over a glass column filled with silica gel (60–120 mesh, 600 g), before being fractionated by repeated chromatography to separate various fractions. The initial elution was carried out with *n*-hexane and the solvent polarity was gradually increased with the addition of EtOAc (3:7 v/v *n*-hexane: EtOAc) to obtained thirty fractions (20 mL) that were minimized to five homogeneous groups (FN_{34}-FN_{38}), whereas FN_{35} (320.3 mg) was fractionated with *n*-hexane: EtOAc (4:1, v/v) to yield compound **1** (120 mg). The purity of compound **1** was ascertained by TLC (silica gel GF_{254}; MeOH: EtOAc, 1:19 v/v, R_f: 0.96) and reverse-phase HPLC (acetonitrile ACN: MeOH, 2:4 v/v) experiments. The fraction FN_{36} was flash chromatographed (Biotage SP1-B1A, Sweden) on a silica gel column (loaded with 230–400 meshed silica gel) by employing a step gradient of EtOAc/*n*-hexane (0–10% EtOAc) to yield a total of ninety fractions (10 mL). Following thin layer chromatography (TLC) analyses, the identical fractions were pooled to obtain five fractions {50 mL, $FN_{36\text{-}(1\text{-}5)}$}. The fraction $FN_{36(2)}$ was flash chromatographed on a column (230–400 meshed silica gel) with EtOAc/*n*-hexane (1:9 to 3:7, v/v) to yield compound **2** {$FN_{36(2)}$, 120.5 mg). The purity of compound **2** was ascertained by TLC {silica gel GF_{254}; MeOH/dichloromethane DCM 1:99 v/v, R_f: 0.80) and reverse-phase HPLC (ACN: MeOH, 1:2 v/v) experiments. The fraction $FN_{36(4)}$ was fractionated with silica gel flash chromatography with EtOAc/*n*-hexane (1:1, v/v), and thereafter with MeOH/DCM (1:9, v/v) to yield fifty fractions (10 mL). Following TLC analyses, the identical fractions were pooled to yield $FN_{45\text{-}1}$ through $FN_{45\text{-}11}$. The fraction $FN_{45\text{-}1}$ was further purified by preparatory silica gel TLC, whereas the plate was eluted with DCM/MeOH (9:1, v/v) to afford compound **3** {$FN_{36(4)}$, 50.5 mg) as major component, and its purity was ascertained by TLC (silica gel GF_{254}; MeOH/ $CHCl_3$ 1:19 v/v, R_f: 0.96) and reverse-phase HPLC (ACN: MeOH, 1:2 v/v) experiments.

Spectral analysis of 1-(3-methoxypropyl)-2-propylcyclohexane (1)

Yellow oil; UV $_{MeOH}$ λ_{max} (log ε): 245 nm (3.26), TLC (Si gel GF_{254} 15 mm; EtOAc/MeOH 19:1, v/v) R_f: 0.96; R_t (HPLC, ACN: MeOH, 2:4 v/v): 12.401 min; IR (vibrational spectra were measured between 4000 to 450 cm^{-1} for KBr pellets, all frequencies were reported in cm^{-1}; the notations for the various motions of atoms within the normal modes were defined as: ν, stretching; δ, bending; ω, wagging; ρ, rocking; τ, torsion; s, symmetric; as, asymmetric): 728.70 (C-H ρ), 1014.67 (C–O ν), 1256.18 (CH_2 ν), 1376.13 (C-H ρ), 1458.14 (C-H δ), 1644.58 (C=C ν), 2857.12, 2923.46 (C–H ν); ^{1}H NMR (500 MHz $CDCl_3$): δ_H 1.26 (2H, m, H-1), 1.26 (2H, m, H-2), 1.26 (2H, m, H-3), 1.62 (2H, m, H-4), 2.32 (1H, m, H-5), 2.04 (1H, m, H-6), 1.42 (2H, m, H-7), 1.72 (2H, m, H-8), 4.29 (2H, t, 6.95 Hz, H-9), 3.67 (3H, s, H-10), 1.25 (2H, m, H-11), 1.31 (2H, m, H-12), 0.88 (3H, t, 7.53 Hz, H-13); ^{13}C NMR (125 MHz, $CDCl_3$): δ_C 29.65 (CH_2, C-1), 27.23 (CH_2, C-2), 29.65 (CH_2, C-3), 37.10 (CH_2, C-4), 33.86 (CH, C-5), 32.38 (CH, C-6), 29.88 (CH_2, C-7), 29.66 (CH_2, C-8), 50.87 (CH_2, C-9), 51.45 (CH_3, C-10), 31.97 (CH_2, C-11), 22.7 (CH_2, C-12), 14.12 (CH_3, C-13); HMBC and ^{1}H-^{1}H-COSY data (Table 1); HR(ESI) MS *m/z* measured value 198.1988 $[M]^+$, calcd for $C_{13}H_{26}O$ 198.1984 (Fig. S10-S19).

Spectral analysis of 3-(methoxymethyl)heptyl 3-(cyclohex-3-enyl)propanoate (2)

Yellowish oil; UV $_{MeOH/DCM}$ λ_{max} (log ε): 238 nm (2.82), 262 nm (2.40); TLC (Si gel GF_{254} 15 mm; MeOH/DCM 1:99, v/v) R_f: 0.80; R_t (HPLC, ACN: MeOH, 2:4 v/v): 14.2681 min; IR (KBr, expressed in cm^{-1}): 724.66 (C–H ρ), 878.09 (C-H δ), 1018.99 (C–H ρ), 1114.25 (C–H δ), 1169.65 (C=C ν), 1249.94 (C–CO–C ν), 1366.49 (C=O ν), 1458.06 (C–H ν), 1743.11 (C=O ν), 2856.12 (C-H ν), 2925.01 (C-H ν); ^{1}H NMR (500 MHz $CDCl_3$): δ_H 1.94 (2H, t, 6.13 Hz, H-1), 5.27 (1H, m, H-2), 5.28 (1H, m, H-3), 2.71 (2H, t, 6.69 Hz, H-4), 1.65 (2H, m, H-5), 1.65 (1H, m, H-6), 1.54 (2H, m, H-7), 2.24 (2H, t, 7.34 Hz, H-8), 4.05 (2H, t, 6.85 Hz, H-10), 1.51 (2H, m, H-11), 2.02 (1H, m, H-12), 4.21 (2H, d, 6.78 Hz, H-13), 3.59 (3H, s, H-14), 1.19 (2H, m, H-15), 1.26 (2H, m, H-16), 1.18 (2H, m, H-17), 0.80 (3H, t, 6.77 Hz, H-18); ^{13}C NMR (125 MHz, $CDCl_3$): δ_C 27.15 (CH_2, C-1), 129.93 (CH, C-2), 129.92 (CH, C-3), 25.5 (CH_2, C-4), 32.73 (CH_2, C-5), 40.19 (CH, C-6), 24.97 (CH_2, C-7), 34.13 (CH_2, C-8), 174.37 (C-9), 62.04 (CH_2, C-10), 37.61 (CH_2, C-11), 31.50 (CH, C-12), 62.20 (CH_2, C-13), 51.43 (CH_3, C-14), 29.56 (CH_2, C-15), 28.82 (CH_2, C-16), 26.34 (CH_2, C-17), 14.11 (CH_3, C-18); HMBC and ^{1}H-^{1}H-COSY data (Table 2); HR(ESI) MS *m/z* measured value 296.2354 $[M]^+$, calcd for $C_{18}H_{32}O_3$ 296.2351 (Fig. S20-S29).

Spectral analysis of 2-ethyl-6-(4-methoxy-2-((2-oxotetrahydro-2*H*-pyran-4-yl)methyl)butoxy)-6-oxohexyl5-ethyloct-4-enoate (3)

Yellow oil; UV $_{MeOH}$ λ_{max} (log ε): 245 nm (3.26); TLC (Si gel GF_{254} 15 mm; MeOH/$CHCl_3$ 1:19, v/v) R_f: 0.96; R_t (HPLC, MeOH: ACN, 2:1 v/v): 14.401 min; IR (KBr, expressed in cm^{-1}): 738.89 (C–H ρ), 1073.42 (C–O ν), 1125.95 (CH_2 wag), 1170.14 (C–O ν), 1280.43 (CH_2 ν), 1369.88 (C–H ρ), 1455.83 (C-H δ), 1589.64 (C=C ν), 1736.56 (C=O ν), 2857.58, 2926.28 (C–H ν); ^{1}H NMR (500 MHz $CDCl_3$): δ_H 0.87 (3H, t, 6.80 Hz, H-1), 1.30 (2H, m, H-2), 2.02 (2H, m, H-3), 5.35 (1H, t, 5.68 Hz, H-5), 2.02 (2H, m, H-6), 2.32 (2H, t, 7.80 Hz, H-7), 4.16 (2H, d, 5.80 Hz, H-9), 1.73 (1H, m, H-10), 1.27 (2H, m, H-11), 1.62 (2H, m, H-12), 2.32 (2H, t, 7.80 Hz, H-13), 4.26 (2H, d, 9.08 Hz, H-15), 2.49 (1H, m, H-16), 1.50 (2H, m, H-17), 1.69 (1H, m, H-18), 2.32 (2H, t, 7.80 Hz, H-19), 4.19 (2H, t, 9.08 Hz, H-21), 1.69 (2H, m, H-22), 1.73 (2H, m, H-23), 4.30 (2H, t, 7.44 Hz, H-24), 3.67 (3H, s, H-25), 1.42 (2H, m, H-26), 0.85 (3H, t, 6.80 Hz, H-27), 2.13 (2H, m, H-28), 0.87 (3H, t, 7.17 Hz, H-29); ^{13}C NMR (125 MHz, $CDCl_3$): δ_C 14.20 (CH_3, C-1), 25.12 (CH_2, C-2), 28.24 (CH_2, C-3), 132.45 (C-4), 130.08 (CH, C-5), 34.11 (CH_2, C-6), 29.67 (CH_2, C-7), 174.56 (C-8), 62.17 (CH_2, C-9), 40.19 (CH, C-10), 29.65 (CH_2, C-11), 28.99 (CH_2, C-12), 24.98 (CH_2, C-13), 168.33 (C-14), 68.24 (CH_2, C-15), 34.39 (CH, C-16), 29.26 (CH_2, C-17), 38.88 (CH, C-18), 32.14 (CH_2, C-19), 173.48 (C-20), 60.14 (CH_2, C-21), 30.78 (CH_2, C-22), 32.73 (CH_2, C-23), 65.68 (CH_2, C-24), 51.42 (CH_3, C-25), 29.85 (CH_2, C-26), 19.70 (CH_3, C-27), 30.07 (CH_2, C-28), 22.80 (CH_3, C-29). HMBC and ^{1}H-^{1}H-COSY data (Table 3); HR(ESI) MS *m/z* measured value 510.3557 $[M]^+$, calcd for $C_{29}H_{50}O_7$ 510.3552 (Fig. S30-S39).

Table 1 NMR spectroscopic data of compound **1** in $CDCl_3$[a]

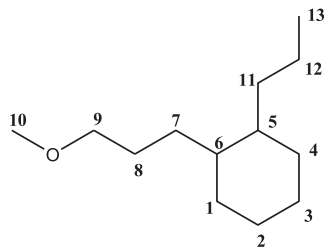

C. No	^{13}C (δ, ppm)	^{1}H-NMR[b] (int., mult., *J* in Hz)	^{1}H-^{1}H COSY	HMBC (^{1}H-^{13}C)
1	29.65	1.26 (2H; m)	-	-
2	27.23	1.26 (2H; m)	-	-
3	29.65	1.26 (2H; m)	4-H	-
4	37.10	1.62 (2H; m)	3-H, 5-H	-
5	33.86	2.32 (1H; m)	4-H, 6-H	-
6	32.38	2.04 (1H; m)	7-H	-
7	29.88	1.42 (2H; m)	6-H	C-5, C-6, C-8
8	29.66	1.72 (2H; m)	9-H	-
9	50.87	4.29 (2H; *J*=6.95 Hz, t)	8-H	C-8
10	51.45	3.67 (3H; s)	-	C-9
11	31.97	1.25 (2H; m)	-	C-12
12	22.7	1.31(2H; m)	-	-
13	14.12	0.88 (3H; *J* =7.53 Hz, t)	12-H	C-11, C-12

[a] NMR spectra recorded using Bruker AVANCE III 500 MHz (AV 500) spectrometer at ambient temperature with TMS as the internal standard (δ 0 ppm).

[b]Values in ppm, multiplicity and coupling constants (*J*= Hz) are indicated in parentheses. The assignments were made with the aid of the ^{1}H-^{1}H COSY, HSQC, HMBC and NOESY experiments.

[a]NMR spectra recorded using Bruker AVANCE III 500 MHz (AV 500) spectrometer at ambient temperature with TMS as the internal standard (δ 0 ppm)

[b]Values in ppm, multiplicity and coupling constants (*J* = Hz) are indicated in parentheses. The assignments were made with the aid of the ^{1}H-^{1}H COSY, HSQC, HMBC and NOESY experiments

Free radical scavenging and anti-inflammatory activities

Radical scavenging potential of the oxygenated meroterpenoids was measured using the 1, 1-diphenyl-2-picrylhydrazyl (DPPH) and 2,2'-azino-bis (3-ethylbenzothiazoline-6-sulphonic acid (ABTS) scavenging assays (Makkar and Chakraborty 2017d). Anti-inflammatory activities were determined by using pro-inflammatory cyclooxygenase-1/2 (COX-1, 2) (Larsen et al. 1996) and 5-lipoxygenase (5-LOX) *in vitro* inhibition assays, as described previously (Baylac and Racine 2003).

Table 2 NMR spectroscopic data of compound **2** in $CDCl_3$[a]

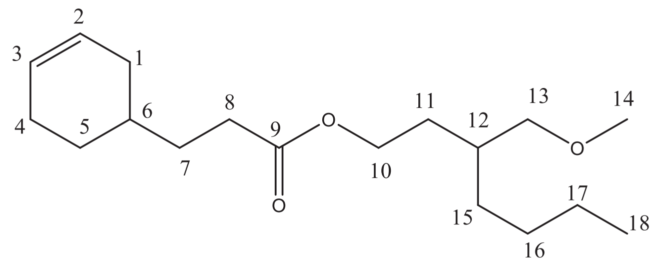

C. No	^{13}C (δ, ppm)	^{1}H-NMR[b] (int., mult., *J* in Hz)	^{1}H-^{1}H COSY	HMBC (^{1}H-^{13}C)
1	27.15	1.94 (t, *J*=6.13 Hz, 2H)	2-H	C-3
2	129.93	5.27 (m,1H)	1-H	C-1
3	129.92	5.28 (m,1H)	4-H	-
4	25.5	2.71 (t, *J*=6.69 Hz, 2H)	3-H	C-3
5	32.73	1.65 (m, 2H)	-	-
6	40.19	1.65 (m, 1H)	-	C-4
7	24.97	1.54 (m, 2H)	8-H	C-9
8	34.13	2.24 (t, *J*=7.34 Hz, 2H)	7-H	C-9
9	174.37	-	-	-
10	62.04	4.05 (t, *J*=6.85 Hz, 2H)	-	-
11	37.61	1.51(m, 2H)	-	-
12	31.50	2.02 (m, 1H)	-	-
13	62.20	4.21 (d, *J*=6.78 Hz, 2H)	-	-
14	51.43	3.59 (s, 3H)	-	-
15	29.56	1.19 (m,2H)	-	C-13
16	28.82	1.26 (m, 2H)	-	C-15
17	26.34	1.18(m, 2H)	-	C-15, C-18
18	14.11	0.80 (t, *J*=6.77 Hz, 3H)	-	C-16

The notations in the table are as under Table 1

Structure–activity relationship analysis

Structure-activity relationship analysis was carried out by applying distinct structural descriptors (ACD Chemsketch, version 8.0 and ChemDraw Ultra version 8.0), named steric {molar volume}, electronic {topological polar surface area (tPSA) and hydrophobic {octanol-water partition coefficient (log P_{ow})} molecular descriptor variables.

Statistical analysis

Statistical analysis was performed with the Statistical Program for Social Sciences 10.0 (SPSS Inc, CA, USA). Analyses were performed in triplicate, and the means of all parameters were assessed for significance ($p \leq 0.05$) by analysis of variance.

Table 3 NMR spectroscopic data of compound **3** in $CDCl_3$[a]

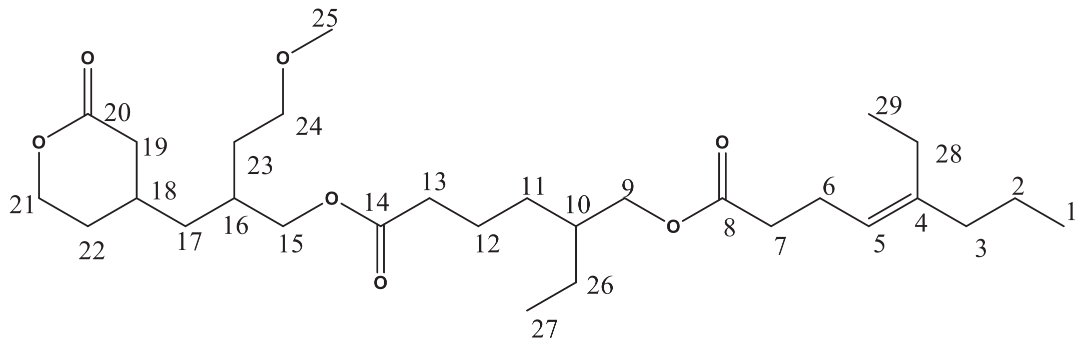

C. No	^{13}C (δ, ppm)	^{1}H-NMR[b] (int., mult., *J* in Hz)	^{1}H-^{1}H COSY	HMBC (^{1}H-^{13}C)
1	14.20	0.87(3H; *J*=6.80 Hz, t)		-
2	25.12	1.30 (2H, m)	-	-
3	28.24	2.02 (2H, m)	-	-
4	132.45	-	-	-
5	130.08	5.35 (1H; *J*=5.68 Hz, t)	6-H	-
6	34.11	2.02(2H, m)	5-H	C-5
7	29.67	2.32(2H; *J*=7.80 Hz, t)	-	C-8
8	174.56	-	-	-
9	62.17	4.16 (2H; *J*=5.80 Hz, d)	-	-
10	40.19	1.73 (1H, m)	-	-
11	29.65	1.27 (2H, m)	12-H	-
12	28.99	1.62 (2H, m)	11-H,13-H	-
13	24.98	2.32 (2H; *J*=7.80 Hz, t)	12-H	-
14	168.33	-	-	-
15	68.24	4.26(2H; *J*=9.08 Hz, d)	-	C-17
16	34.39	2.49(1H, m)	-	-
17	29.26	1.50(2H, m)	-	-
18	38.88	1.69 (1H, m)	-	-
19	32.14	2.32 (2H; *J*=7.80 Hz, t)	-	C-20, C-17
20	173.48	-	-	-
21	60.14	4.19 (2H; *J*=9.08 Hz, t)	-	C-20
22	30.78	1.69 (2H, m)	-	-
23	32.73	1.73 (2H, m)	24-H	-
24	65.68	4.30 (2H, *J*=7.44 Hz, t)	23-H	-
25	51.42	3.67 (3H; s)	-	-
26	29.85	1.42 (2H, m)	-	C-10
27	19.70	0.85 (3H; *J*=6.80 Hz, t)		
28	30.07	2.13 (2H; m)	-	-
29	22.80	0.87 (3H; *J*=7.17 Hz, t)	-	-

The notations in the table are as under Table 1

Results and discussion

Spectral analyses of meroterpenoids from *K. alvarezii*

1-(3-Methoxypropyl)-2-propylcyclohexane (compound **1**), a methoxy-substituted C_{13} meroterpenoid, was purified as yellow oil by extensive column chromatography on adsorbent silica gel. The mass spectrum displayed the molecular ion peak at *m/z* 198 (Fig. S1) enclosing mono unsaturation (because of the ring system), and the molecular formula as $C_{13}H_{26}O$ based upon combined ^{1}H and ^{13}C NMR spectral data (Table 1). The existence of 13 carbon signals constituting of nine methylenes, two methines and one each of methoxy and methyl carbons was supported by the ^{13}C NMR experiment (Table 1). The deshielded resonance of H-9 (δ_H 4.29, $J = 6.95$ Hz) of **1** suggested the C-9 methylene groups remained attached to an electronegative group, possibly of oxygenated origin. The ^{1}H-^{1}H COSY correlations were observed between δ_H 2.32 (H-5)/ δ_H 2.04 (H-6); δ_H 1.62 (H-4)/ δ_H 2.32 (H-5) were apparent, and were ascribed to the cyclohexane ring framework (Fig. 2, Fig. S2). The methine (–CH) carbon signals were apparent at δ_C 33.86 (C-5) and C-6 (δ_C 32.38) that appropriately recognized the junction point of cyclohexane ring system substituted with propane and the methoxypropane moieties, respectively. HMBC correlations from δ_H 1.25 (assigned as H-11) to δ_C 22.7 (C-12); δ_H 1.42 (H-7) to δ_C 33.86 (C-5)/ δ_C 31.97 (C-6)/ δ_C 29.66 (C-8); δ_H 0.88 (H-13) to δ_C 31.97 (C-11)/ δ_C 22.7 (C-12); δ_H 4.29 (H-9) to δ_C 29.66 (C-8); δ_H 3.67 (H-10) to δ_C 50.87 (C-9) displayed the side chain substitutions of the cyclohexane ring system. In addition, ^{1}H-^{1}H COSY correlations appeared at δ_H 4.29 (H-9)/ δ_H 1.72 (H-8), δ_H 2.04 (H-6)/ δ_H 1.42 (H-7), which were due to the 1-methoxypropane framework attached to the cyclohexane ring system, and was in accordance with the J^{1-3} HMBC attributions. Similarly, ^{1}H-^{1}H COSY correlation appeared at δ_H 1.31 (H-12)/ δ_H 0.88 (H-13), which was due

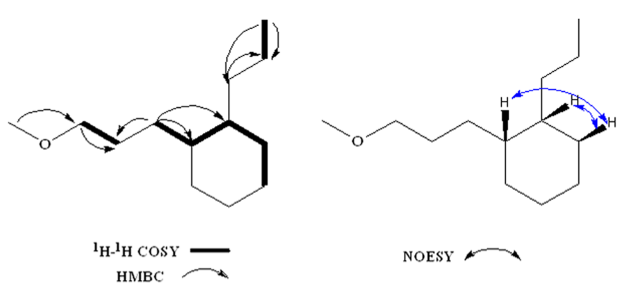

Fig. 2 a Key ^{1}H-^{1}H COSY, HMBC and NOESY correlations of compound **1**. The ^{1}H-^{1}H COSY cross peaks were displayed by bold face bonds, whereas the selected HMBC correlations were shown as double barbed arrows. The β orientation in the NOESY relations was presented as blue coloured arrows

to the framework attached to the cyclohexane ring system. The combined ^{1}H/ ^{13}C NMR demonstrated highly deshielded oxymethylene protons at δ_H 4.29 (attributed to H-9) corresponding to the carbon resonance at δ_C 50.87 (C-9) to assign the propylcyclohexane ring system and side chain substitution in C_{13} meroterpenoid. The relative stereochemistries of **1** were attributed by NOESY experiments. The reference plane of the compound **1** was arbitrarily chosen as the cyclohexane ring system. NOESY cross peaks between δ_H 2.32 (H-5)/ δ_H 1.62 (H-4) suggested their close proximity, and therefore, assigned to align on an identical plane of the cyclohexane ring system with di-equatorial β-faced interaction. Intense NOESY cross peaks between δ_H 1.62 (H-4)/ δ_H 2.04 (H-6) appropriately indicated their equiplaner disposition (β-orientation).

3-(Methoxymethyl)heptyl 3-(cyclohex-3-enyl)propanoate (compound **2**), an oxygenated C_{18} meroterpenoid displayed the molecular ion peak at *m/z* 296 (Fig. S4) enclosing three degrees of unsaturation {due to the ester carbonyl group (δ_C 174.37), olefinic carbon at δ_C 129.92 (C-3), δ_C 129.93 (C-2) and a ring system}, and the molecular formula as $C_{18}H_{32}O_3$ based upon combined ^{1}H and ^{13}C NMR spectral data (Table 2). The IR-spectrum of **2** displayed the presence of carbonyl group along with olefinic groups due to the bands recorded at 1458 and 2856 cm^{-1}. The ^{13}C NMR spectrum established the existence of 18 carbon signals constituting eleven methylene, two methine, along with one each of carbonyl, olefinic, methyl and methoxy carbons. The ^{1}H NMR in combination with ^{13}C NMR experiments demonstrated highly deshielded oxymethylene protons at H-10 (δ_H 4.05, $J = 6.85$ Hz) and H-13 (δ_H 4.21, $J = 6.78$ Hz) that were deduced to be correlated with the corresponding carbon signals at C-10 and C-13 methylene groups, and that was further corroborated based on the existence of an ester carbonyl {δ_C 174.37 (C-9)} and sharp singlet (integral of three) of O–CH_3 group in the NMR spectrum. The ^{1}H-^{1}H COSY correlations between δ_H 1.94 (denoted as H-1)/ δ_H 5.27 (H-2) and δ_H 5.28 (assigned to H-3)/ δ_H 2.71 (H-4) were ascribed to the cyclohexane ring framework (Fig. S5). The J^{1-3} HMBC correlation between δ_H 1.94 (denoted as H-1) to δ_C 129.92 (C-3), δ_H 5.27 (H-2) to δ_C 27.15 (C-1) and δ_H 2.71 (H-4) to δ_C 129.92 (C-3) attributed the presence of cyclohexene ring system. The methine (–CH) carbon at C-6 (δ_C 40.19) recognized the junction of cyclohexene ring moiety and was substituted with 3-(methoxymethyl) heptyl butyrate skeleton (Fig. S6). This was corroborated by the ^{1}H–^{1}H COSY and J^{1-3} HMBC correlations. HMBC cross peaks between δ_H 1.54 (assigned as H-7) to δ_C 174.37 (C-9), δ_H 2.24 (H-8) to δ_C 174.37 (C-9) appropriately supported the presence of ester carbonyl carbon attached to the cyclohexene ring system. Additional J^{1-3} HMBC correlations were displayed between δ_H 1.19 (assigned to H-15) to δ_C 62.20 (C-13), δ_H 1.26 (H-16) to δ_C

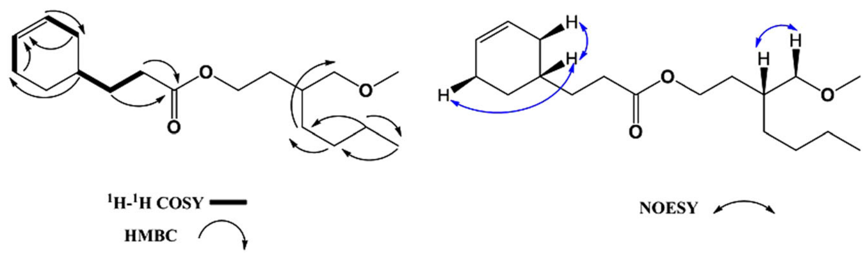

Fig. 3 a Key ^{1}H-^{1}H COSY, HMBC and NOESY correlations of compound **2**. The ^{1}H-^{1}H COSY cross peaks were displayed by bold face bonds, whereas the selected HMBC correlations were shown as double barbed arrows. The β orientation in the NOESY relations was presented as blue coloured arrows

29.56 (C-15), δ_H 1.18 (H-17) to 29.56 (C-15)/ 14.11 (C-18), δ_H 0.80 (H-18) to δ_C 28.82 (C-16), which apparently indicated the substitution of 3-(methoxymethyl)heptyl butyrate to the cyclohexene ring system. The methoxy group was found to appear as a singlet at δ_H 3.59 (attributed to H-14; HSQC δ_C 51.43 at C-14) to support the presence of 3-(methoxymethyl) heptyl butyrate framework. In addition, the olefinic group was found to appear as the multiplet at δ_H 5.27–5.28 (H2-H3) {HSQC, δ_C 129.93 (C-2), δ_C 129.92 (C-3)}, which attributed to the cyclohexene ring framework. The chemistries of the stereogenic centres bearing protons were derived using NOESY-assisted relative stereochemical assignments . An intense NOESY correlation was displayed between the protons at δ_H 1.65 (H-6) and δ_H 1.94 (H-1; J = 6.13 Hz)/ and δ_H 2.71 (H-4; J = 6.69 Hz), which suggested their equi-planer disposition, and was arbitrarily attributed as β-oriented. Strong NOESY correlation between δ_H 2.02 (H-12; J = 6.69 Hz) and δ_H 4.21 (H-13; J = 6.78 Hz) attributed the protons to dispose at the β-side of the reference plane, which suggested their diaxial orientation with reference to the plane of the symmetry (Fig. 3).

2-Ethyl-6-(4-methoxy-2-((2-oxotetrahydro-2*H*-pyran-4-yl)methyl)butoxy)-6-oxohexyl-5-ethyloct-4-enoate (compound **3**), a highly oxygenated C_{29} meroterpenoid, was purified as yellowish oil with *m/z* 510 (Fig. S7) bearing five degrees of unsaturation, and its structure was characterized by combined ^{1}H and ^{13}C NMR spectral experiments (Table 3). The IR bending vibration near 1736 cm^{-1} was associated with the carbonyl group, whereas the olefinic groups were assigned to the absorption bands at 1455 and 2857 cm^{-1}. The ^{13}C NMR spectroscopic data deduced the existence of 29 carbon signals constituting three each of methyl, methylene and ester carbonyl groups along with seventeen methylene and one each of olefinic and methoxy carbons. The ^{1}H NMR in combination with ^{13}C NMR demonstrated highly deshielded oxymethylene protons at δ_H 4.16 (attributed to H-9, J = 5.80 Hz), 4.19 (H-21, J = 9.08 Hz), 4.26 (H-15, J = 9.08 Hz) and 4.30 (H-24, J = 7.44 Hz) in the proton spectrum suggesting that the C-24, C-21, C-15 and C-9 methylene groups were attached to an electronegative group, possibly of oxygenated origin. This was further corroborated by the presence of ester carbonyl carbons {δ_C 174.56 (assigned to C-8), δ_C 168.33 (C-14), δ_C 173.48 (C-20)} and a singlet (integral of three) of O-CH_3 group {δ_C 51.42 (C-25)}, in the NMR spectrum. The proton-proton connections were apparent between δ_H 1.73 (ascribed to H-23)/ δ_H 4.30 (H-24) that assigned the part of a tetrahydro-2*H*-pyran-2-one ring framework. The $J^{1\text{-}3}$ HMBC correlations between δ_H 2.32 (ascribed to H-7) to δ_C 174.56 (C-8), δ_H 4.26 (H-15) to δ_C 29.26 (C-17), δ_H 4.19 (H-21) to δ_C 173.48 (C-20) and δ_H 2.32 (H-19) to δ_C 29.26 (C-17)/ 173.48 (C-20) appropriately deduced the existence of highly deshielded oxymethylene protons and ester carbonyl carbon as part of the tetrahydro-2*H*-pyran-2-one ring framework. The ^{1}H–^{1}H COSY correlation between δ_H 1.27 (ascribed to H-11)/ δ_H 1.62 (H-12)/ δ_H 2.32 (H-13) were probably attributed to the part of substituted tetrahydro-2*H*-pyranone ring system (Fig. 3, Fig. S8). In addition, an olefinic group was found to appear as the multiplet at δ_H 5.35 (H-4/H-5) {HSQC, δ_C 132.45 (C-4) and δ_C 130.08 (C-5)}, which was situated at the extended side chain of **3**. The ^{1}H-^{1}H correlation between δ_H 5.35 (denoted as H-5)/ δ_H 2.02 (H-6) and a HMBC correlation between δ_H 2.02 (assigned as H-6) to δ_C 130.08 (C-5) appropriately established the existence of the olefinic group. The HMBC correlation from δ_H 1.42 (assigned as H-26) to δ_C 29.85 (C-10) deduced the substitution of 2-ethyl-6-(2-ethyl-4-methoxybutoxy)-6-oxohexyl 5-ethyloct-4-enoate to the pyran-2-one ring system in **3**. The methoxy group was found to appear as singlet at δ_H 3.67 {attributed to H-25; HSQC δ_C 51.42 (C-25)}, which described the 2-ethyl-6-(2-ethyl-4-methoxybutoxy)-6-oxohexyl 5-ethyloct-4-enoate framework. The relative stereochemistries of the stereogenic centres in **3** were deduced by NOESY experiments. NOESY cross peaks at δ_H 1.69 (H-18)/ δ_H 4.19 (H-21; J = 9.08 Hz)/ δ_H 2.32 (H-19; J = 7.80 Hz) appropriately suggested their close proximity and equi-planer orientation (arbitrarily assigned to β-faced). NOESY correlation between the di-

Table 4 Antioxidative and anti-inflammatory activities of the meroterpenoids isolated from *K. alvarezii vis-à-vis* the commercial agents

Pharmacological activities {IC_{50} (mg/mL)}

Antioxidative activities*	**Compound 1**	**2**	**3**	**BHA**	**BHT**	**α-tocopherol**
DPPH· scavenging	$0.70^a \pm 0.01$	$0.52^a \pm 0.06$	$0.31^a \pm 0.03$	$0.26^b \pm 0.01$	$0.25^b \pm 0.02$	$0.63^c \pm 0.04$
$ABTS^{+\cdot}$ scavenging	$0.72^a \pm 0.11^a$	$0.58^a \pm 0.15^a$	$0.34^a \pm 0.13^a$	$0.34^b \pm 0.02$	$0.26^b \pm 0.02$	$0.73^c \pm 0.05$
Anti-inflammatory activities*	**Compound 1**	**2**	**3**	**Aspirin**	**Na-salicylate**	**Ibuprofen**
COX -1 inhibition	$1.20^a \pm 0.03$	$1.18^a \pm 0.04$	$1.12^a \pm 0.02$	$0.005^a \pm 0.00$	$1.93^c \pm 0.05$	$0.04^a \pm 0.00$
COX -2 inhibition	$1.09^a \pm 0.06$	$1.08^a \pm 0.09$	$1.05^a \pm 0.07$	$0.21^b \pm 0.02$	$2.65^c \pm 0.05$	$0.09^a \pm 0.02$
Selectivity Index**	$1.10^a \pm 0.06$	$1.09^a \pm 0.09$	$1.06^a \pm 0.07$	$0.02^b \pm 0.02$	$0.72^c \pm 0.05$	$0.44^a \pm 0.02$
5-LOX inhibition	$1.14^a \pm 0.05$	$1.10^a \pm 0.04$	$1.04^a \pm 0.02$	$0.39^a \pm 0.02$	$1.75^c \pm 0.12$	$0.93^b \pm 0.11$

*The bioactivities were expressed as IC_{50} values (mg/mL). The samples were analyzed in triplicate ($n = 3$) and expressed as a mean ± standard deviation. Means followed by the different superscripts (a–c) within the same row indicate significant differences ($P < 0.05$)

**Selectivity index has been calculated as the ratio of anti-COX-1(IC_{50}) to that of anti-COX-2 (IC_{50})

equatorial protons at δ_H 4.30 (H-24; $J = 7.44$ Hz)/ δ_H 2.49 (H-16) apparently attributed to their close spatial arrangements, and therefore, were assigned to be at the β-face with reference to the molecular plane of symmetry. Likewise, an intense NOESY correlation was observed between δ_H 1.73(H-10)/ δ_H 1.27 (H-11) that implied their deposition on the same side of the plane with di-axial interaction (Fig. 4, Fig. S8).

Structure–activity relationship analysis

The radical scavenging and anti-inflammatory properties of the oxygenated meroterpenoids isolated from *K. alvarezii* were compared with commercially available synthetic standards (Table 4). The highly oxygenated C_{29} meroterpenoid **3** displayed potential antioxidative activities as determined by ABTS and 1, 1-diphenyl-2-picryl-hydrazil (DPPH) free radical scavenging potential ($IC_{50} < 0.35$ mg/mL), and was comparable with those exhibited by α-tocopherol (IC_{50} 0.6–0.7 mg/mL, $P < 0.05$). The electron-delocalization between the carbonyl, methoxy, and olefinic bonds in the molecular structure of these compounds might probably contribute towards the potential free radical scavenging properties (Pietta 2000; Cai et al. 2006). These title meroterpenoid derivatives showed significantly greater inhibition towards the inducible COX-2 than its constitutive cyclooxygenase isoform, and accordingly, their anti-inflammatory selectivity index (SI, anti-COX-1_{IC50}/anti-COX-2_{IC50}) were lower (1.06–1.10) than synthetic NSAIDs (ibuprofen and aspirin, SI: 0.44 and 0.02, respectively; $P <$ 0.05). In particular, no significant variation in the *in vitro* inhibitory activities towards pro-inflammatory 5-lipoxidase (IC_{50} 1.04–1.14 mg/mL) and cycloxygenase-2 (IC_{50} 1.05–1.09 mg/mL) of compound **3** indicated its potential anti-inflammatory properties against inducible inflammatory mediators causing an inflammatory response. Notably, sodium salicylate appeared to be a weaker inhibitor of the COX isoforms (anti-COX-2 IC_{50} 2.65 mg/mL, anti-COX-1 IC_{50} 1.93 mg/mL), and exhibited significantly lesser activity against 5-LOX (anti-LOX-5 IC_{50} 1.75 mg/mL) (Table 4).

The radical quenching along with cyclooxygenase and lipoxygenase inhibitory activities of the meroterpenoids were determined by lipophilic (log P_{ow}, octanol-water partition-coefficient), steric (molar refractivity, MR) and electronic (tPSA, topological polar surface area) parameters. The radical quenching and anti-inflammatory properties of the studied compounds were found to be directly related to their hydrophobic characters as determined by hydrophobicity-lipophilicity balance (log P_{ow}). A greater value of log P_{ow} indicated the higher molecular hydrophobicity. The compound **1** showed lesser hydrophobicity (log P_{ow} 4) than those displayed by **2** (log P_{ow} 4.26) and **3** (log P_{ow} 5.46). The hydrophobic property was deduced to ascribe the inter-membrane permeability of a compound, the optimal range being 2–5 for appropriate lipophilic–hydrophobic characteristics (Lipinski and Hopkins 2004). The decreased activity of compound **1** might be corroborated with the lesser hydrophobicity and reduced membrane permeability. Resultantly, the lipophilic DPPH radical might easily be associated with meroterpenoids possessing greater hydrophobicity (greater log P_{ow} value) and displaying higher radical scavenging property. On the basis of above attribution, it might be ascribed that the electronic and hydrophobic factors play significant roles to narrate the bioactive potential of the studied compounds. The electron-rich centers were found to constitute the methoxy-substituted side chain, hydroxyl and aryl substituents in the ring framework. These groups might possibly function as the centre of unsaturations, and were attributed to potential anti-inflammatory and radical quenching properties of the meroterpenoids. The aggregate number of electronegative centres and centre of unsaturation were lesser in **1**, thereby resulting in lesser activity than those

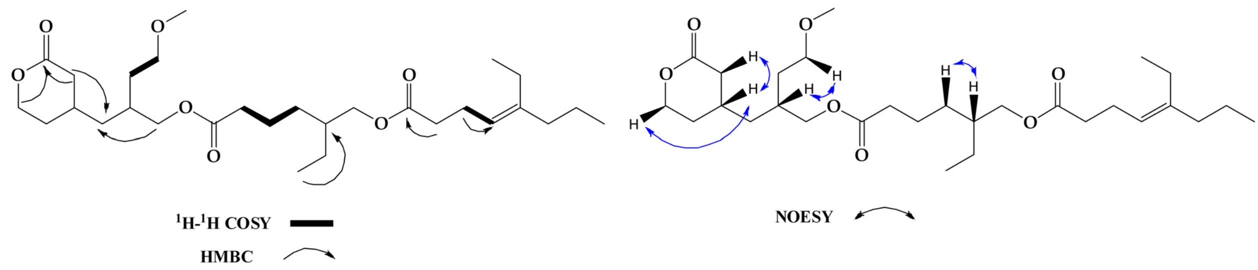

Fig. 4 Key ^{1}H-^{1}H COSY, HMBC and NOESY correlations of compound **3**. The ^{1}H-^{1}H COSY cross peaks were displayed by bold face bonds, whereas the selected HMBC correlations were shown as double barbed arrows. The β orientation in the NOESY relations was presented as blue coloured arrows

recorded in compounds **2** and **3**. The optimum log P_{ow} of the highly oxygenated C_{29} meroterpenoid **3** (~5.46) along with greater topological polar surface area (tPSA 88.13) might result in its potential anti-inflammatory activity in terms of inhibiting COX-2 (IC_{50} 1.05 mg/mL) and 5-LOX (IC_{50} 1.04 mg/mL) (Table 4).

Conclusions

Three oxygenated meroterpenoids, characterized as 1-(3-methoxypropyl)-2-propylcyclohexane **(1)**, 3-(methoxymethyl)heptyl 3-(cyclohex-3-enyl)propanoate **(2)** and 2-ethyl-6-(4-methoxy-2-((2-oxotetrahydro-2*H*-pyran-4-yl) methyl)butoxy)-6-oxohexyl 5-ethyloct-4-enoate **(3)** were purified from the ethyl acetate-methanol fraction of the intertidal red seaweed *K. alvarezii*. The highly oxygenated C_{29} meroterpenoid **3** with potential radical quenching and anti-inflammatory potential might qualify this compound as candidate pharmacological lead against oxidative stress and inflammation.

Acknowledgements Financial support from the Science and Engineering Research Board (SERB) of Department of Science and Technology, Ministry of Science and Technology in the form of research grant (SR/S1/OC-96/2012 SERB) is gratefully acknowledged. The authors thank the Director, Central Marine Fisheries Research Institute, for his guidance and support. Thanks are due to the Head, Marine Biotechnology Division, Central Marine Fisheries Research Institute for facilitating the research activity. FM acknowledges Department of Science and Technology, for the award of fellowship.

Compliance with ethical standards

Conflict of interest The authors declare that they have no conflict of interest.

References

Areche C, Benites J, Cornejo A, Ruiz LM, García-Beltrán O, Simirgiotis MJ, Sepúlveda B (2015) Seco-taondiol, an unusual meroterpenoid from the Chilean seaweed *Stypopodium flabelliforme* and its gastroprotective effect in mouse model. Mar Drugs 13:1726–1738

Ask EI, Azanza RV (2002) Advances in cultivation technology of commercial eucheumatoid species: a review with suggestions for future research. Aquacult 206:257–277

Baylac S, Racine P (2003) Inhibition of 5-lipoxygenase by essential oils and other natural fragment extracts. Int J Aromather 13:138–142

Cai YZ, Mei S, Jie X, Luo Q, Corke H (2006) Structure-radical scavenging activity relationships of phenolic compounds from traditional Chinese medicinal plants. Life Sci 78:2872–2888

Chakraborty K, Joseph D, Joy M, Raola VK (2016) Characterization of substituted aryl meroterpenoids from red seaweed *Hypnea musciformis* as potential antioxidants. Food Chem 212:778–788

Chandrasekaran S, Nagendran AN, Pandiaraja D, Krishnankutty N, Kamalakannan B (2008) Bioinvasion of *Kappaphycus alvarezii* on corals in the Gulf of Mannar, India. Curr Sci 94:1167–1172

Ebada SS, Lin WH, Proksch P (2010) Bioactive sesterterpenes and triterpenes from marine sponges: occurrence and pharmacological significance. Mar Drugs 8:313–346

Gershenzon J, Dudareva N (2007) The function of terpene natural products in the natural world. Nat Chem Biol 3:408–414

Larsen LN, Dahl E, Bremer J (1996) Peroxidative oxidation of leuco-dichloroluorescein by prostaglandin H synthase in prostaglandin biosynthesis from polyunsaturated fatty acids. BBA Lipid Met 1299:47–53

Liebgott T, Miollan M, Berchadsky Y, Drieu K, Culcasi M, Pietri S (2000) Complementary cardioprotective effects of flavonoid metabolites and terpenoid constituents of *Ginkgo biloba* extract (EGb 761) during ischemia and reperfusion. Basic Res Cardiol 95:368–377

Lipinski C, Hopkins A (2004) Navigating chemical space for biology and medicine. Nature 432:855–861

Makkar F, Chakraborty K (2017a) Unprecedented antioxidative cyclic ether from the red seaweed *Kappaphycus alvarezii* with anti-cyclooxygenase and lipoxidase activities Nat Prod Res 31 (10):1131–1141

Makkar F, Chakraborty K (2017b) Antidiabetic and anti-inflammatory potential of sulphated polygalactans from red seaweeds *Kappaphycus alvarezii* and *Gracilaria opuntia* Int J Food Prop 20 (6):1326–1337

Makkar F, Chakraborty K (2017c) Antioxidative sulfated polygalactans from marine macroalgae as angiotensin-I converting enzyme inhibitors. Nat Prod Res. https://doi.org/10.1080/14786419.2017.1363756.

Makkar F, Chakraborty K (2017d) Previously undescribed antioxidative azonicyl morpholinone alkaloid from red seaweed *Gracilaria opuntia* with anti-cyclooxygenase and lipoxidase properties. Nat Prod Res 32(10):1150–1160

Parshikov IA, Netrusov AI, Sutherland JB (2012) Microbial transformation of antimalarial terpenoids. Biotechnol Adv 30:1516–1523

Pietta PG (2000) Flavonoids as antioxidants. J Nat Prod 63:1035–1042

Reis VM, Oliveira LS, Passos RMF, Viana NB, Mermelstein C, Sant'Anna C, Pereira RC, Paradas WC, Thompson FL, Amado-Filho GM, Salgado LT (2013) Traffic of secondary metabolites to cell surface in the red alga *Laurencia dendroidea* depends on a two-step transport by the cytoskeleton. PLoS One 8:63929

Zbakh H, Talero E, Avila J, Alcaide A, de los Reyes C, Zubía E, Motilva V (2016) The algal meroterpene 11-hydroxy-11-O-methylamentadione ameloriates dextran sulfate sodium-induced colitis in mice. Mar Drugs 14:149